applied sciences

MDPI

Article

Palpreast—A New Wearable Device for Breast Self-Examination

Lucia Arcarisi [1,2], Licia Di Pietro [1,2], Nicola Carbonaro [1,2], Alessandro Tognetti [1,2,*], Arti Ahluwalia [1,2] and Carmelo De Maria [1,2,*]

[1] Research Center E. Piaggio, University of Pisa, Largo Lucio Lazzarino 1, 56122 Pisa, Italy; lu.arcarisi@gmail.com (L.A.); dipietrolicia@gmail.com (L.D.P.); nicola.carbonaro@unipi.it (N.C.); arti.ahluwalia@unipi.it (A.A.)

[2] Department of Information Engineering, University of Pisa, Via G. Caruso 16, 56122 Pisa, Italy

* Correspondence: alessandro.tognetti@unipi.it (A.T.); carmelo.demaria@unipi.it (C.D.M.)

Received: 18 September 2018; Accepted: 17 January 2019; Published: 22 January 2019

Abstract: Breast cancer is the most commonly diagnosed cancer in women worldwide. Although targeted screening programs using mammography have facilitated earlier detection and improved treatment has resulted in a significant reduction in mortality, some negative aspects related to cost, the availability of trained staff, the duration of the procedure, and its non-generalizability to all women must be taken into consideration. Breast palpation is a simple non-invasive procedure that can be performed by lay individuals for detecting possible malignant nodules in the breast. It is a simple test, based on the haptic perception of different stiffness between healthy and abnormal tissues. According to a survey we carried out, despite being safe and simple, breast self-examination is not carried by women because they are not confident of their ability to detect a lump. In this study, a non-invasive wearable device designed to mimic the process of breast self-examination using pressure sensing textiles and thus increase the confidence and self-awareness of women is proposed. Combined with other screening methods, the device can increase the odds of early detection for better prognosis. Here, we present the physical implementation of the device and a finite element analysis of the mechanics underlying its working principle. Characterization of the device using models of large and medium breast phantoms with rigid inclusions demonstrates that it can detect nodules in much the same way as does the human hand during breast self-examination.

Keywords: breast cancer; breast self-examination; breast palpation; pressure sensing textile; wearable device

1. Introduction

Breast cancer is the most commonly diagnosed cancer in women worldwide. With more than 1 million cases in 2012 [1], it is one of the most common causes of cancer-related death in women [2]. It is estimated that 1 woman in 8 will develop breast cancer during her life, but this estimation varies by country; in Italy for example, 50,000 new cases are discovered each year [3,4].

The incidence of breast cancer is strongly related to age with the highest incidence rates being in menopausal women. Breast cancer in women under 40 years is not a common condition; however, the increase of incidence in premenopausal women is particularly alarming. Premenopausal women are not commonly covered by national screening programs, and often a mammography cannot be performed because of the high density of their breast tissue [5–8]. Breast cancer can be suspected under different circumstances, such as a positive screening mammography or echography, discovery by palpation of a mass in the breast, or any morphological modification of the breast. Currently, the most widely used clinical diagnostic method is mammography. Even though mammography screening has

been successful in reducing mortality, in particular in women over 50, some negative aspects related to cost, the availability of trained staff, the duration of the test, and the non-applicability to all women must be considered. In fact, despite being the gold standard of diagnostic techniques, mammography cannot be used on pregnant women because of ionizing radiation. This technique is also ineffective in young dense breasts [7]. Moreover, as a routine diagnostic tool, mammography is costly, placing an economic load on already overburdened healthcare systems. There is, therefore, a need for low-cost, reliable early detection method for breast cancer, particularly in the younger population.

Currently, several products are available in the market in support of early detection. They are generally used for clinical breast examination (CBE) by physicians to perform their work and hence are not wearable [9,10]. These devices, through tactile imaging, take advantages of the different mechanical properties of the tissues in order to detect anomalies located inside the breast. Tactile imaging is a new emerging diagnostic technique based on visualizing the sense of touch. Biological tissues are characterized by specific mechanical properties, which change in the course of the lump's development. Using these features, it is possible to create pressure maps in relation to the direction of tissue deformation. This is because the pressure response corresponding to areas with abnormalities is higher than the healthy tissue. Considering the effectiveness of this simple and risk-free methodology, several devices imitate the haptic process performed during palpation using different types of technologies, such as ultrasound or pressure sensors. Among the advantages of using tactile sensors instead of human touch are their greater reliability and repeatability [10–13].

According to a study performed by Egorov et al. [10], tactile imaging showed a sensitivity of 91.4% and specificity of 86.1% on a sample of 32 malignant lesions and 147 benign ones. These results are comparable to the effectiveness of other diagnostic techniques but tactile imaging has several advantages, such as ease of use, portability, absence of radiation, and lower costs. The low cost is, above all, what makes the procedure interesting as a method for screening particularly in countries with limited resources where high technology techniques are not available.

Breast self-examination (BSE) [14] is the most common method of early-stage breast cancer detection. The sensitivity of BSE is related to significant changes in mechanical properties of tissue in the course of cancer development. BSE, or regularly examining one's own breasts, could be used to find early signs of breast cancer, when it is more likely to be treated successfully. It is a simple non-invasive procedure that can be performed by all women, allowing them to become comfortable with their own bodies [15]. Self-palpation should be performed once a month, several days after the beginning of menstruation when the breasts are softer. A woman palps her breast with the pads of her finger to detect either superficial or deeper lumps. The breast is assumed to be divided into four quadrants, each of which is checked separately. Several common patterns are designed to ensure complete coverage of the breast also including "the axillary tail" (the piece of breast tissue which extends under the armpit) [14].

A number of wearable systems in support of BSE are already patented and commercialized. Among these, thermal technology, which estimates thermal maps of the breast using infrared sensors, is the most common. Other examples of intelligent bras show additional parameters such as the differences between oxygenated and non-oxygenated hemoglobin, and the evaluation of the levels of oxygenation, which have a different distribution in healthy and diseased tissues [16–19]. Diseased tissue is in fact characterized by a higher metabolism and therefore develops areas with higher temperature.

In this study, we present a non-invasive wearable device named Palpreast to simulate breast self-examination using pressure sensing textiles. As far as we know, the use of the tactile of technology on a wearable device to provide a tool for home screening has not been proposed, as all current devices are based on different techniques (heat and oxygen levels). Palpreast is not conceived to be a diagnostic tool but as a support that, in combination with other screening methods, can increase the odds of early detection for better prognosis.

In the following sections, we outline the results of a survey conducted to better understand the reasons why women do not practice BSE. The device concept is introduced, and then the finite element (FE) analysis of the mechanics underlying the working principle is presented. The physical implementation of the device and its characterization are discussed. Finally, the proposed solution is validated using a breast phantom with an embedded inclusion.

2. Survey

We evaluated the level of awareness that women have about the impact of the breast cancer, and the practice of BSE. The main focus is to understand why women are not confident about practicing breast palpation despite the fact that it is simple and safe. The questionnaire was submitted to a sample of 1169 Italian women, aged between 15 and 82 years with different levels of education as shown in Figure 1.

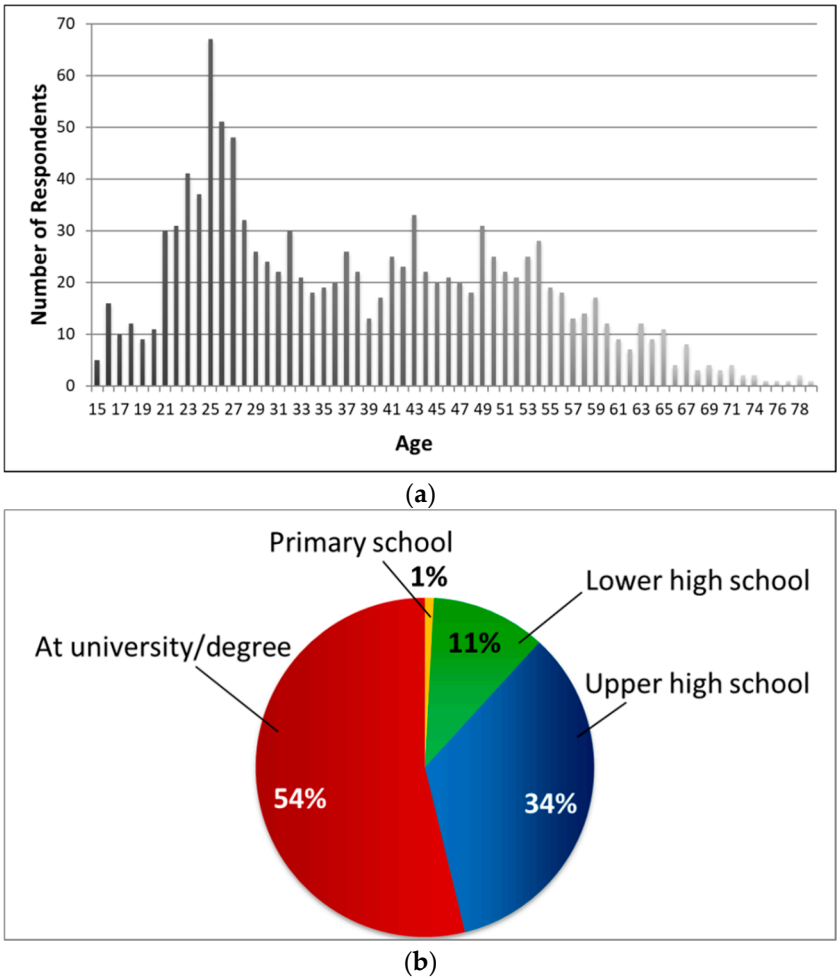

Figure 1. Questionnaire. (**a**) Age distribution of the samples involved in the questionnaire. (**b**) Pie chart of the percentages of the sample based on their level of education.

The main results from the questionnaire show a lack of awareness of the incidence of breast cancer. Only 27% of women know how high the incidence of breast cancer is, while only 19% of them practice BSE correctly and on a regular basis (Figure 2). From the questionnaire, the lack of confidence in their own ability to detect lump was the main reason why women do not practice self-palpation.

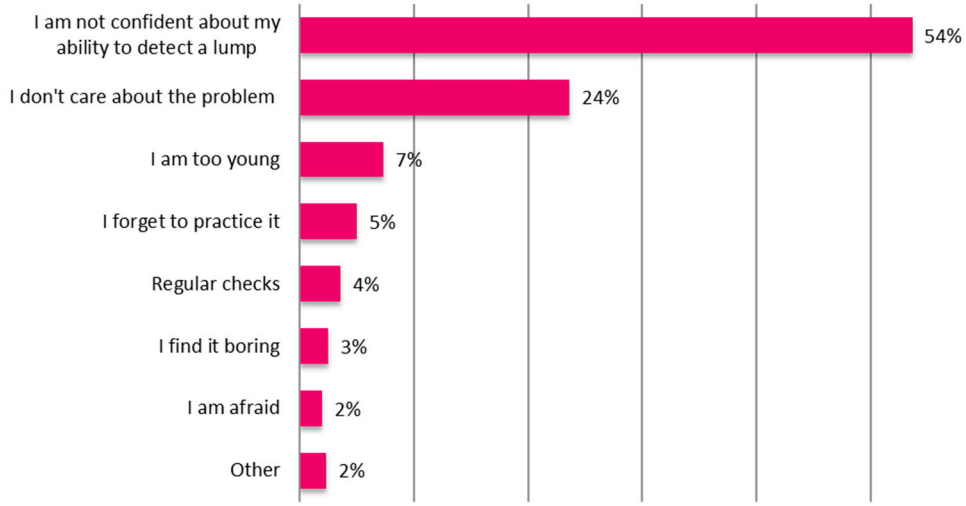

Figure 2. Questionnaire results—percentage of responses to the question "Why don't you practice breast self-examination (BSE)?"

The most worrying outcome of our survey is that the least aware age group is the one that is most at risk, i.e., premenopausal women.

3. Device Concept

Palpreast is a wearable device similar to a stretchy bra (Figure 3a), with an internal pocket, adaptable to breasts with different shapes and sizes. A pressure sensing textile responsible for nodule detection is located under the stretchy top, in contact with the skin (Figure 3b). An inflation system, composed of four independent air compartments centered on the breast, is located in the inner part of the top (see Figure 3c).

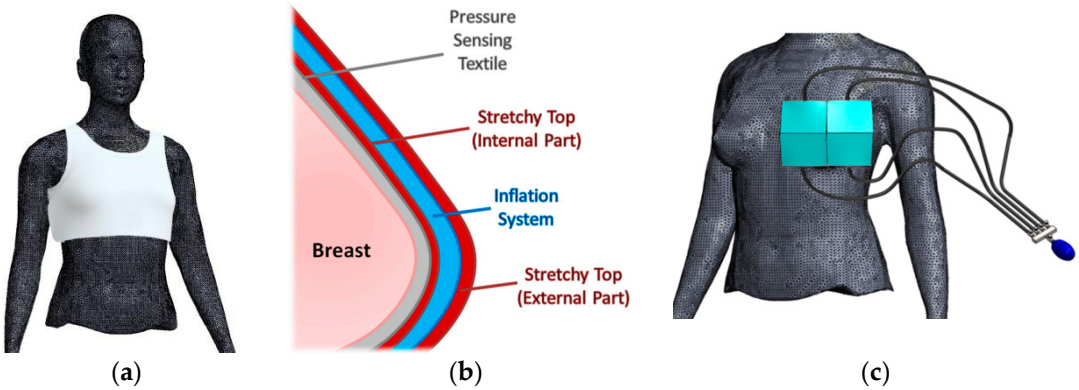

Figure 3. Palpreast conceptual design—(**a**) external top; (**b**) internal layer view; and (**c**) inflation system.

The working principle of the device is based on a pressure sensing textile able to distinguish tissue stiffness, thus differentiating between healthy and abnormal tissue. The textile covers the breast and the inflator system separately inflates and deflates each of the four compartments allowing the sensing textile to adhere sequentially to the breast, simulating the process of self-examination. An intuitive graphical interface presents the result of the difference in stiffness region-by-region between the left and right breast, which can be an indicator of the presence of a malignant nodule (considering that it is highly improbable to have two identical nodules in the left and right breast, with the same stiffness and in the same position). With this strategy, the contralateral breast constitutes the internal control, without the need for further calibration. According to this conceptual design, the proposed wearable device, as explained in Section 1, is not intended to be a diagnostic tool, but is conceived as a support

for BSE promoting the detection of the early stage of disease for improving its prognosis. The device was developed according to the approach proposed by the EU funded UBORA project [20,21], which aimed at developing open source medical devices compliant to European Medical Device Regulation 2017/745.

4. Finite Element Analysis

A finite element (FE) analysis of a breast model was performed to investigate its response to a compression load, in order to demonstrate the feasibility of the idea and determine the technical specifications to design the prototype of Palpreast, e.g., the spatial resolution of the pressure sensing textile necessary to identify the presence of a nodule.

Mechanical properties of tissues are highly sensitive to the structural changes of various physiological and pathological processes. Thus, the characterization of embedded lesions in terms of mechanical properties (such as stiffness and size) provides a means for distinguishing them from diseased tissues. Although women have different breast thickness, shape, and stiffness, the FE analysis is based on a simplified hemispherical breast model characterized by average mechanical properties and a reduced number of details (e.g., heterogeneous tissues). This choice derives from the device concept, which is based on the evaluation of the differences in stiffness between the right and left breast—healthy heterogeneous tissues present in both breasts should have the same behavior, whereas there may be substantial differences between healthy and diseased tissues of the same person.

In order to define the Young's modulus of the breast and the nodule, we took into account the study of Egorov et al. [12], which was based on the application of a similar technology and on in vivo studies on patients. According to this study, the Young's modulus of healthy breast tissue was 7 kPa, calculated as the mean value of clinical data of six patients involved in the study (6.9 ± 1.4 kPa). Tumors are in general stiffer than healthy tissue, and it is well known that the Young's modulus increases with the malignancy of a tumor [22,23]. In this research, we performed a parametric analysis with respect to the Young's modulus of the inclusion E_{nod}, in the range 50 to 125 kPa with a step of 25 kPa, according to the in vivo study performed in [12], where the elastic modulus of inclusions increased from 50 kPa (benign fibrocystic tissue) to 123 kPa (ductal carcinoma).

Two-dimensional (2D) plane strain and three-dimensional (3D) brick models were implemented under the following assumptions:

1. The biological tissue and inclusions were homogeneous, linear elastic, and isotropic;
2. The Poisson's ratio of each material is 0.45, i.e., the breast could be considered as an almost incompressible material;
3. The breast was assumed to be placed on a non-deformable hard surface (identifiable with the rib cage), with a no-displacement constraint as boundary condition;
4. The density of each material was set to 1000 kg/m^3 (close to the density of water);
5. Two different breast sizes were investigated—large breast (LB) and medium breast (MB);
6. The ideal breast tissue has a hemispherical shape, whereas the nodule has a spherical shape, whose dimensions are indicated in Figure 4 and Table 1 for 2D model, and Figure 5 and Table 2 for the 3D model;
7. A pressure of 10 kPa was considered to simulate breast palpation.

All the FE simulations were modeled using COMSOL Multiphysics 3.5.

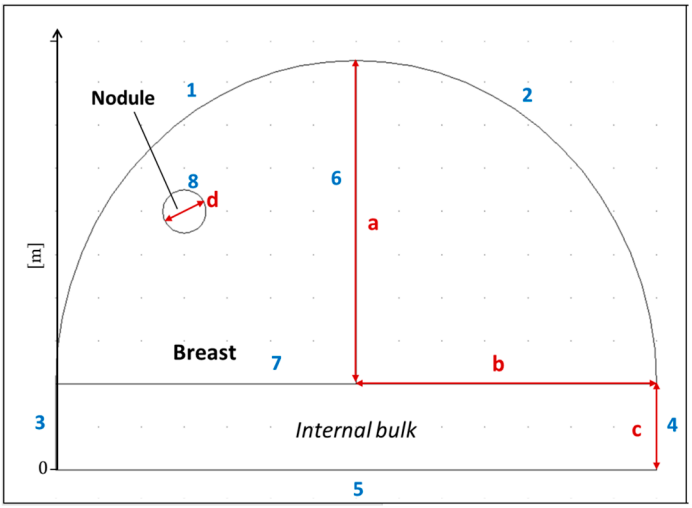

Figure 4. Two-dimensional (2D) model with 10-mm diameter inclusion embedded in breast tissue (large breast, LB). Blue numbers indicate the boundary of the breast, while red letters define the breast's dimensions. A description of the parameters is given in Table 1.

Table 1. Model parameters for the 2D finite element (FE) analysis. The expressions "nx_pn" and "ny_pn" are internal variables of COMSOL to describe the normal direction with respect to the indicated boundary.

Nodule Position (Center)	LB [m]	MB [m]
x	−0.045	−0.03
y	0.055	0.04
Variable	**[m]**	**[m]**
a	0.07	0.05
b	0.14	0.1
c	0.02	0.015
d	0.01	0.01
Mesh Elements Degree of Freedom (DoF)	914 3758	790 3270

Boundary Number	Boundary Condition
1	Load Fx = −10000*nx_pn [Pa] Fy = −10000*ny_pn [Pa]
5	Constraint Rx = 0, Ry = 0
2,3,4,6,7,8	No Constraint

In order to simulate the behavior of breast tissue with better accuracy, a FE analysis of an idealized 3D breast model (Figure 5) was performed considering the parameters described in Table 2. The dimensions were the same as the 2D models described in Table 1.

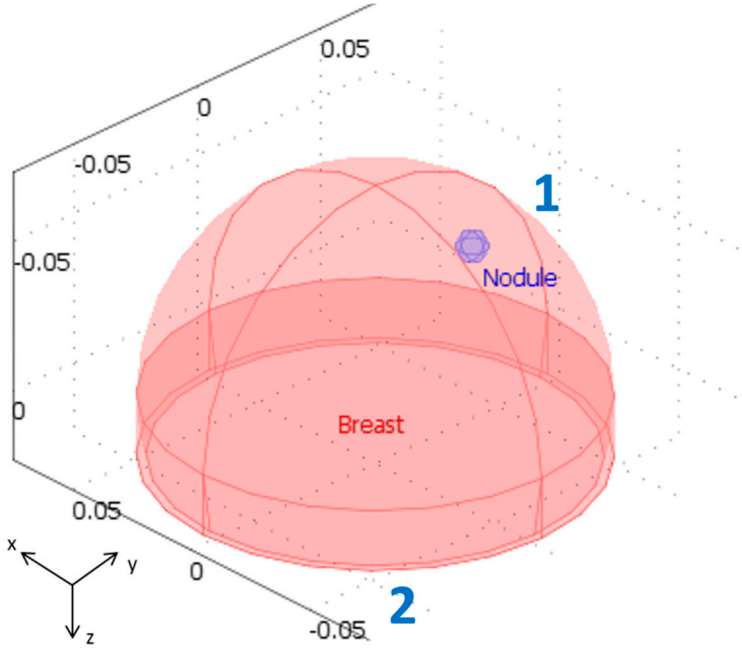

Figure 5. Three-dimensional (3D) model for FE analysis with 10-mm diameter inclusion embedded in breast tissue (LB) (Axes are in (m)).

Table 2. Model parameters for the 3D FE analysis.

Nodule Position (Center)	LB [m]	MB [m]
x	−0.02	0.01
y	0.02	0.02
z	−0.05	−0.03
Mesh Elements Degree of Freedom (DoF)	9320 41,328	8635 38,355

Boundary Number	Boundary Condition
1	Load Fx = −10000*nx_pn [Pa] Fy = −10000*ny_pn [Pa] Fz = −10000*ny_pn [Pa]
2	Constraint Rx = 0, Ry = 0, Rz = 0
Other elements	No Constraint

Figure 6 represents the total displacement in response to an external pressure on the 2D breast model—according to the model, the maximum difference in displacement between healthy and abnormal breast tissue ranges from 2.5 mm up to 3 mm depending on the Young's modulus of the inclusion. Figure 7 highlights the total displacement of boundary #1 of the 2D breast model for different positions of the inclusion—the position of the maximum difference in displacement between a healthy and abnormal breast changes with the position of the inclusion, and reaches a higher value when the inclusion is closer to the surface of the breast.

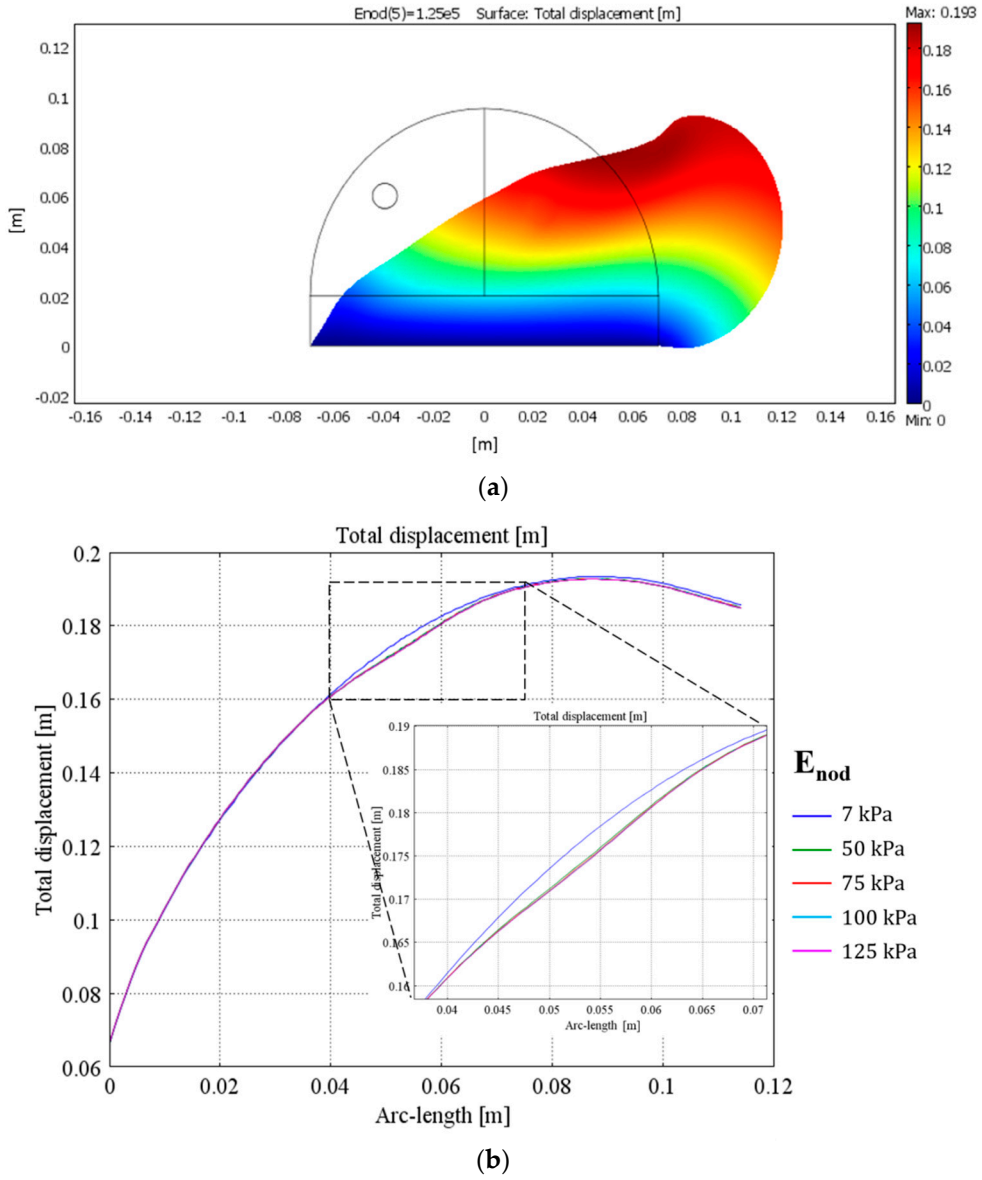

Figure 6. Displacement field of the LB 2D model, with a 10 mm diameter inclusion and an applied pressure of 10 kPa. (**a**) Surface plot of the displacement with an inclusion with E_{nod} = 125 kPa; and (**b**) total displacement plot of boundary #1 of the breast for different E_{nod} values. The blue line shows the response of a healthy breast.

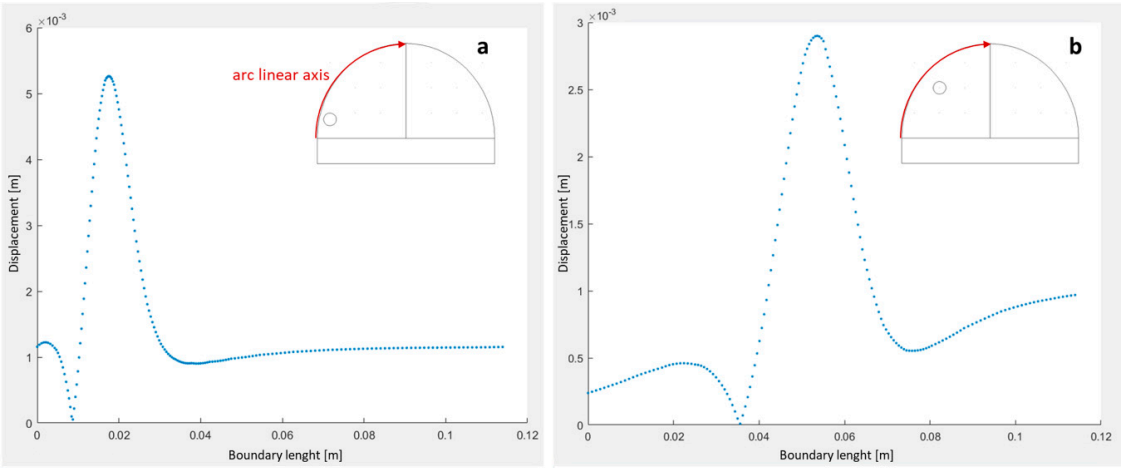

Figure 7. Differential displacement between abnormal and healthy breast as a function of nodule position evaluated along the boundary #1, indicated in red in the inset. (**a**) 125 kPa nodule placed superficially and closer to the boundary (see inset); and (**b**) 125 kPa nodule placed deeper in the breast and near the center (see inset).

The 3D FE model was used to evaluate the spatial resolution necessary to clearly identify the presence of the inclusion (Figure 8).

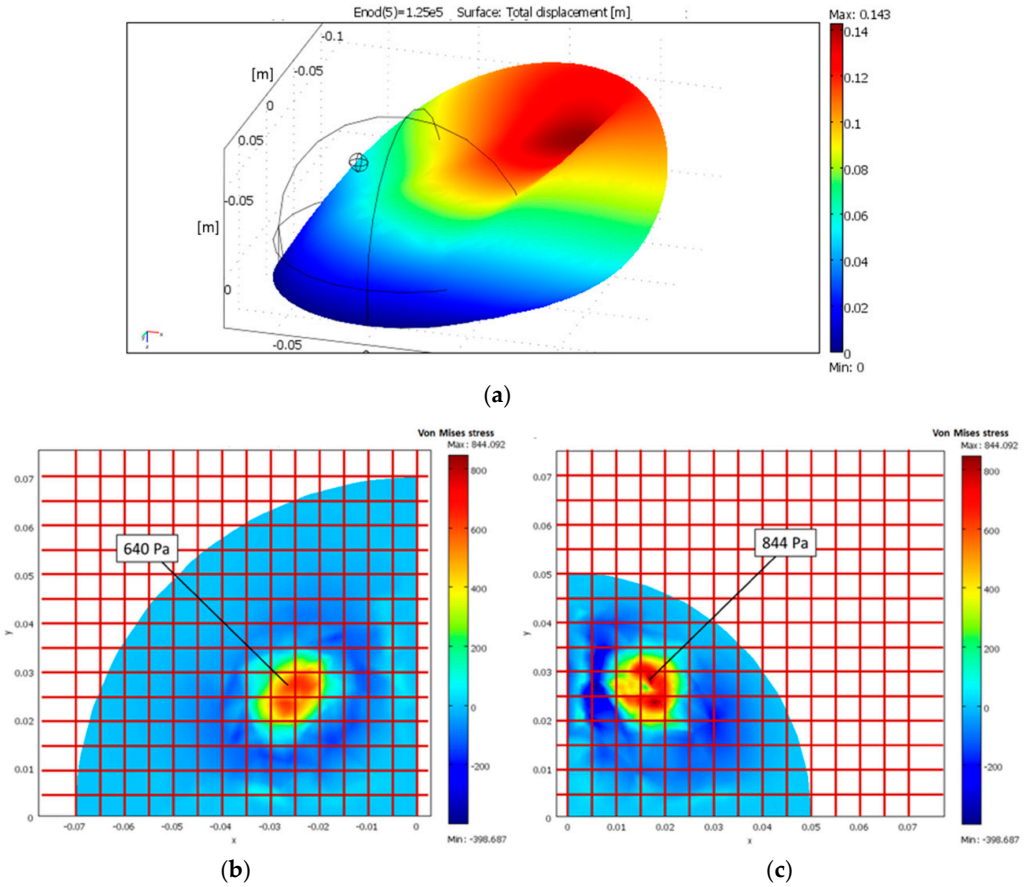

Figure 8. (**a**) Total displacement in the 3D FE model of the breast with a 10-mm inclusion with Young's modulus of 125 kPa. The 2D map of the Von Mises stress with a superimposed 5 mm spaced grid for LB (**b**) and medium breast (MB) model (**c**). The bar scale is in (Pa).

According to the 3D FE model, differences in the Von Mises stress between the healthy and abnormal tissue (Figure 8b,c) indicated that a sensor matrix able to detect a change in pressure of 600 Pa over a distance of 5 mm was sufficient to detect the presence of a stiffer inclusion of 10-mm diameter located inside a breast. The analysis also suggested that as the size of breast increased, the pressure gradient due to inclusion decreased (lower variation), i.e., detecting an inclusion in a smaller breast was easier than in a larger one.

5. Device Implementation

5.1. Textile Pressure Sensing Matrix

A textile pressure sensing matrix was designed using a multilayer textile structure. This multi-pressure sensing structure is inspired by previous studies on textile-based pressure sensors [24] and is sketched in Figure 9a. A continuous layer of piezoresistive textile (stretchable fabric manufactured by Eeonyx (http://eeonyx.com/, US), surface resistivity of 10^5 Ω/m^2, see Figure 9b) is placed between two layers of fabric having custom-designed highly conductive stripes (stretchy zebra fabric produced by Eeonyx, where the width of conductive stripes is 24 mm and the insulating stripes is 6 mm). As shown in Figure 9a, the top and bottom conductive patterns are perpendicular. Each intersection between a row (top layer) and a column (bottom layer) represents a sensing element (taxel). On applying a force on a taxel, the conductive layer gets compressed and the density of the conductive particles increases, causing the resistance to decrease. The number of taxels (i.e., sensing areas) is given by the product of the number of rows and the number of columns.

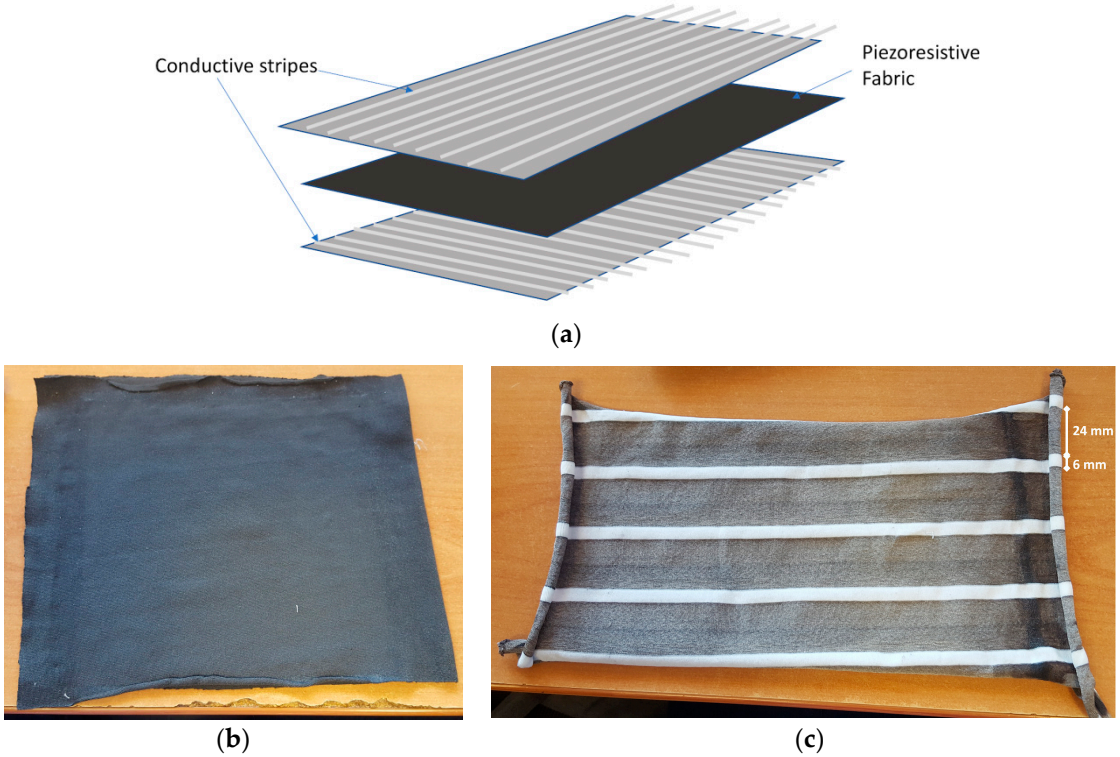

(**a**)

(**b**) (**c**)

Figure 9. (**a**) Multi-pressure sensing structure; (**b**) piezoresistive fabric; and (**c**) zebra-patterned conductive fabric.

Figure 10 presents the pressure sensing matrix with its physical model, implementation, and graphical interface. The acquisition system, based on the Arduino DUE board, was designed to sequentially select all the taxels of the matrix and to measure their electrical resistance—rows were selected by sequentially providing the 3.3 V to each strip using the Digital Ports (D in Figure 10) of the microcontrollers, while the four columns were identified through four different analog ports

(A in Figure 10). The change in resistance, related to the applied force, was converted to voltage by a voltage-resistance divider, with the fixed resistance of 10 kΩ, and the voltage signal was digitized by an analog-to-digital converter (12-bit ADC) integrated with the Arduino DUE board. A firmware designed with Arduino IDE was uploaded on the Arduino board, and the digital values of the matrix were transmitted through the serial port. An appropriate interface, designed with processing, was used to interpret the magnitude of pressure through a matrix system represented by a heat map that replicated the sensor matrix structure.

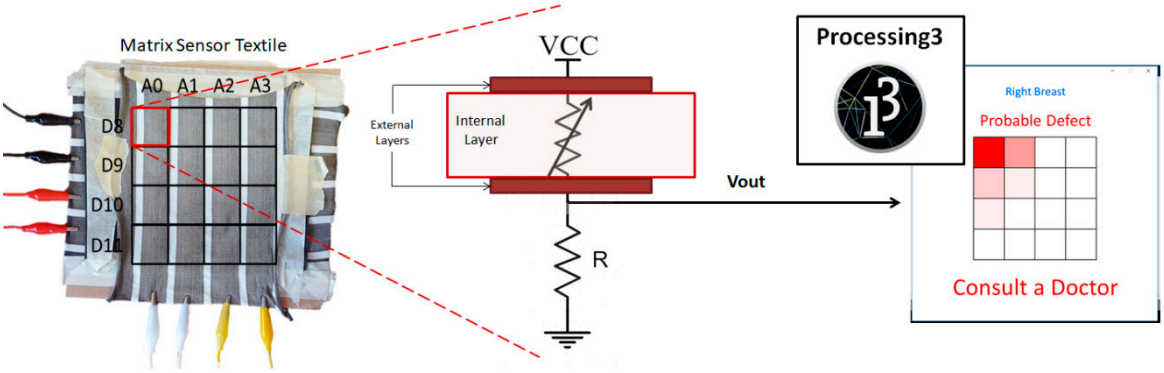

Figure 10. Pressure sensing matrix—physical model, implementation, and graphical interface. VCC: 3.3 V.

5.2. Actuation System

The textile pressure sensing matrix and the inflator system are contained in a stretchy top used by women for chest protection in martial arts (see Figure 11a), which totally covers the breast, up to the axillary zones. The top has an internal pocket where a rigid protective structure is located to prevent an excessive expansion of the inflator system.

The inflator system, inserted between the layers and composed of four compartments of 70 mm × 80 mm each, allows the adhesion of the sensor to the breast one quadrant at a time. The inflator system consists of a bulb pump with related air release valve, a manometer to check the pressure, and an appropriately designed structure with T valves to control the air flux in each compartment. In this way, balloons inserted in each compartment and connected to the pumping system through rubber hoses are inflated (see Figure 11b). The assembled Palpreast is shown in Figure 11c.

(**a**) (**b**) (**c**)

Figure 11. Palpreast prototype—(**a**) stretchy top with a rigid protective structure; (**b**) inflator system; and (**c**) assembled system.

6. Device Characterization

6.1. Sensing Matrix Calibration

The textile pressure sensing matrix was calibrated using different weights (2, 3, 4, 10, 20, 40, and 70 g) placed, one at time, on each taxel (16 in total in a 4 rows (R) × 4 columns (C) matrix; each taxel is indicated in the text with the coordinates Rn,Cn with n varying between 0 and 3) for 5 seconds before signal acquisition from all taxels. All weights had the same contact area with the matrix (470 mm^2), which was used to calculate the applied pressure. Tests were performed in triplicate.

6.2. Phantom Fabrication

A breast phantom was purposely developed for testing the device's ability to detect a stiffer inclusion within a healthy tissue. A healthy phantom was fabricated by casting silicone Ecoflex 00-10 (Smooth-on, Inc, Macungie, PA, USA) with the addition of three parts of Slacker additive (Smooth-on, Inc, Macungie, PA, USA) into a custom-made open mold of the breast. The design of the mold was based on a realistic model of the human breast developed with the 3D computer graphics software MakeHuman (www.makehumancommunity.org), and built with Fortus 250mc FDM 3D printer (Stratasys, Eden Prairie, MN, USA, 2013). Silicone was prepared according to the manufacturer's instructions to have a final Young's modulus of 7 kPa, corresponding to healthy tissue.

The diseased breast phantom was prepared with the same protocol as the healthy one with the addition of a stiffer inclusion (irregular shape, approximately spherical, with a Feret diameter of 2 cm), separately prepared with the silicone Dragon Skin 10 (Smooth-on, Inc, Macungie, PA, USA), which has a Young's modulus of 180 kPa. The inclusion was inserted into the mold containing Ecoflex during its polymerization (Figure 12).

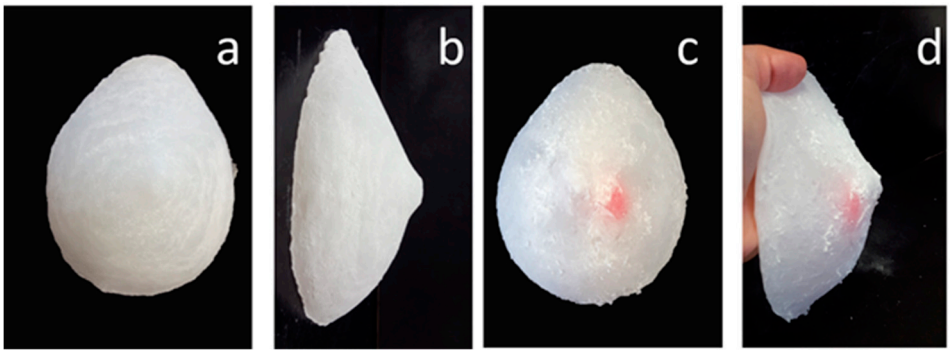

Figure 12. Breast phantoms—healthy breast (**a**,**b**); and abnormal breast (**c**,**d**).

6.3. Nodule Identification Test Protocol

To verify the ability of the pressure sensor matrix to identify the presence of a nodule inside the breast, the healthy and abnormal breast phantoms were pressed with an increasing load onto the sensor matrix, which was suspended on a rigid frame. Phantoms were placed in different positions and different loads were applied. Signals from all taxels were acquired for 10 s with a sampling rate of 0.5 Hz, and the median value was calculated. Between two different measurements, the rest value (absence of phantom) was acquired for excluding possible displacement of the fabric layers.

7. Characterization Results

The textile pressure sensing matrix was highly reproducible, with a limited standard deviation (fractional standard deviation <1.18%). A typical response is illustrated in Figure 13, showing the digital output of all taxels resulting from the application of different pressures (load weight ÷ taxel area) on taxel R0,C0. We observed substantial crosstalk within taxels of the same column but no significant crosstalk with taxels of different columns.

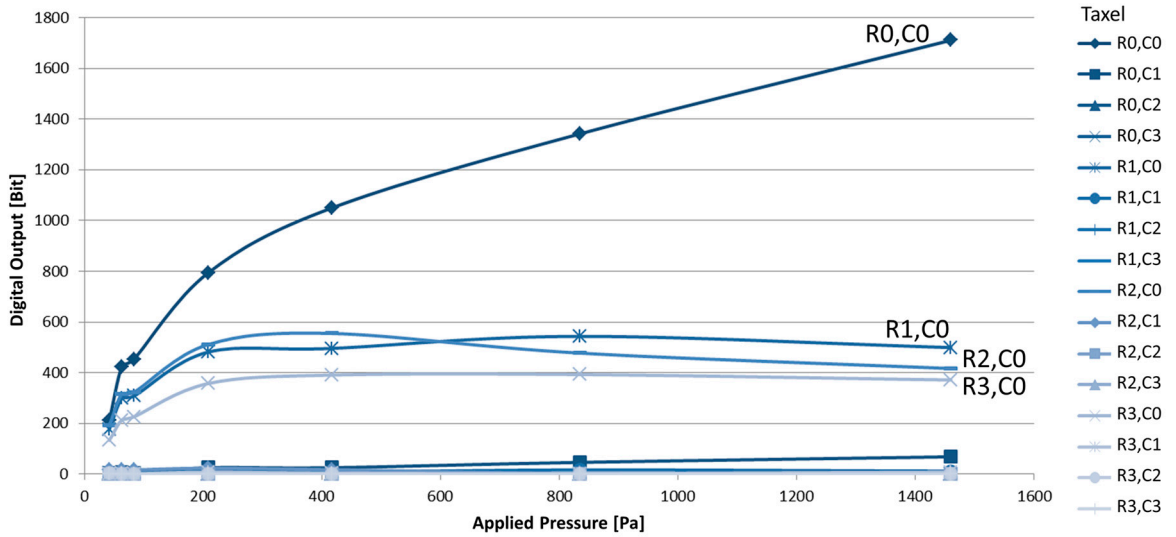

Figure 13. Example of textile pressure sensing matrix response after the application of different pressures in position (R0,C0).

The ability of the device to identify the presence of a stiffer inclusion in the breast phantom is demonstrated in Figure 14, where the results of pressing the phantoms with a fixed load against the matrix is shown: the difference between healthy and abnormal breast gives different values of the acquired signals. Similar behavior was observed for other positions of the phantoms.

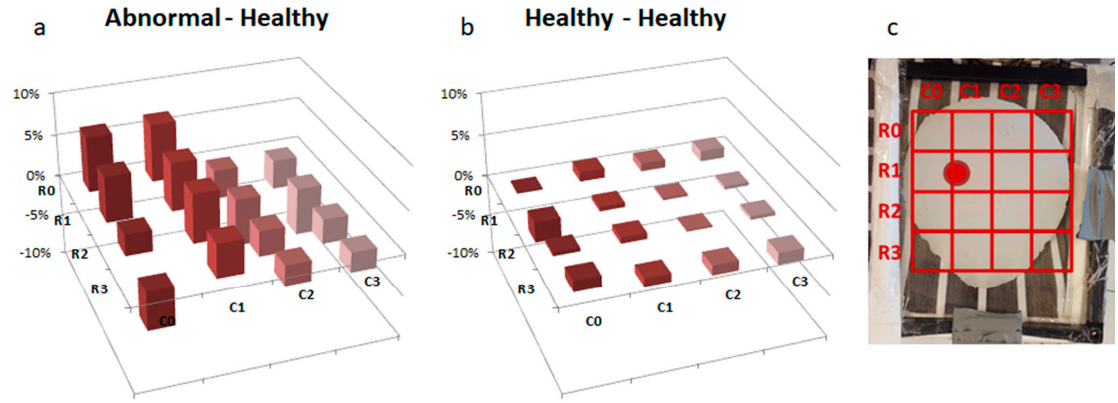

Figure 14. Ability of the textile pressure sensing matrix to detect the presence of a stiffer inclusion at R1,C0-R1,C1 in the breast phantom. The phantoms were pressed with a load of 672 Pa against the matrix. (**a**) Differences (in %) between healthy–abnormal acquisition; (**b**) differences (in %) of two acquisitions with two healthy phantoms; and (**c**) position of the inclusion during the registration.

8. Conclusions

We present a wearable device—Palpreast—for breast self-examination based on tactile imaging. The device was modelled using FE analysis, and then designed, assembled, and tested using breast phantoms. It consists of a stretchy top which covers both breasts, with internal layers consisting of (a) wearable sensors (n.b., although the prototype is constructed using piezo resistive fabric, other pressure or displacement sensing materials (e.g., piezo capacitive) could also be used in the device); (b) a compartment containing sub-compartments which can be selectively inflated by applying a precise pressure to different zones of the breast. Alternate inflation of each subcompartment mimics the action of breast palpation and the resulting haptic feedback detected by the wearable sensors gives an indication of the difference in stiffness between the left and right breast, which are correlated to the

size and location of nodules; (c) an intelligent interface for analysis of differences in stiffness between the left and right breast giving appropriate alerts to users to consult a doctor.

Results from the calibration of the system indicate that it is highly reproducible although we did observe some crosstalk between taxels. More sophisticated data analysis, using, for example, a neural network, could overcome this limitation and even take advantage of this crosstalk [25]. Despite this limit in resolution, the device in its current form is able detect the presence of a 2 cm nodule in a breast phantom.

As Palpreast can be classified as a Class I medical device according to Medical Device Regulation 2017/745 (low risk, not being a diagnostic tool), it does need to undergo clinical trials. However, further improvements on the FE analysis using reconstructed 3D images of real breasts would be useful to understand how non-symmetrical shapes of the breast or irregular contours of the nodule may influence the resolution of the system, and thus if a sensor pad with smaller and more densely packed taxels is required. In addition, miniaturization of the pneumatic system as well as preliminary tests on a number of volunteers is necessary for the device to be marketed as a support for personal screening in women.

Author Contributions: L.A. conceived the device. All authors contributed to its modeling, design, realization, and testing as well as to the preparation and editing of the manuscript.

Funding: This project has received funding from the European Union's Horizon 2020 research and innovation programme under grant agreement No 731053 UBORA.

Acknowledgments: The authors would like to acknowledge the "PhD+" and "Contamination Lab" programs of the University of Pisa, and the Additive Manufacturing CrossLab of the Department of Information Engineering of the University of Pisa for the support in development of the idea of wearable device for breast self-examination. The device is named "Palpreast" after the programs "PhD+" and "Contamination Lab" at the University of Pisa, devoted to the incubation of innovative ideas toward product development.

Conflicts of Interest: The authors declare no conflict of interest. The funders had no role in the design of the study; in the collection, analyses, or interpretation of data; in the writing of the manuscript, or in the decision to publish the results.

References

1. Ferlay, J.; Soerjomataram, I.; Dikshit, R.; Eser, S.; Mathers, C.; Rebelo, M.; Parkin, D.M.; Forman, D.; Bray, F. Cancer incidence and mortality worldwide: Sources, methods and major patterns in GLOBOCAN 2012. *Int. J. Cancer* **2015**, *136*, E359–E386. [CrossRef] [PubMed]
2. U.S. Breast Cancer Statistics. Available online: https://www.breastcancer.org/symptoms/understand_bc/statistics (accessed on 14 July 2018).
3. American Cancer Society. How Common Is Breast Cancer? Available online: https://www.cancer.org/cancer/breast-cancer/about/how-common-is-breast-cancer.html (accessed on 12 July 2018).
4. Associazione Italiana di Oncologia Medica; Associazione Italiana dei Registri Tumori. *I numeri del cancro in Italia*; Il Pensiero Scientifico: Roma, Italy, 2017.
5. Cardoso, F.; Loibl, S.; Pagani, O.; Graziottin, A.; Panizza, P.; Martincich, L.; Gentilini, O.; Peccatori, F.; Fourquet, A.; Delaloge, S.; et al. The European Society of Breast Cancer Specialists recommendations for the management of young women with breast cancer. *Eur. J. Cancer* **2012**, *48*, 3355–3377. [CrossRef] [PubMed]
6. Samphao, S.; Wheeler, A.J.; Rafferty, E.; Michaelson, J.S.; Specht, M.C.; Gadd, M.A.; Hughes, K.S.; Smith, B.L. Diagnosis of breast cancer in women age 40 and younger: Delays in diagnosis result from underuse of genetic testing and breast imaging. *Am. J. Surg.* **2009**, *198*, 538–543. [CrossRef] [PubMed]
7. Nover, A.B.; Jagtap, S.; Anjum, W.; Yegingil, H.; Shih, W.Y.; Shih, W.H.; Brooks, A.D. Modern breast cancer detection: A technological review. *J. Biomed. Imaging* **2009**, 26. [CrossRef] [PubMed]
8. Carioli, G.; Malvezzi, M.; Rodriguez, T.; Bertuccio, P.; Negri, E.; La Vecchia, C. Trends and predictions to 2020 in breast cancer mortality in Europe. *Breast* **2017**, *36*, 89–95. [CrossRef] [PubMed]
9. Sure. Sure Touch. 2017. Available online: https://suretouch.us/ (accessed on 11 July 2018).
10. Sarvazyan, A.; Egorov, V.; Sarvazyan, N. Tactile sensing and tactile imaging in detection of cancer. *Biosens. Mol. Technol. Cancer Diagn.* **2012**, 337–352.

11. Yousuf, M.A.; Asiyanbola, B.A. A review of force and resonance sensors used in the clinical study of tissue properties. *Proc. Inst. Mech. Eng. Part H J. Eng. Med.* **2013**, *227*, 1333–1340. [CrossRef] [PubMed]
12. Egorov, V.; Sarvazyan, A.P. Mechanical imaging of the breast. *IEEE Trans. Med. Imaging* **2008**, *27*, 1275–1287. [CrossRef] [PubMed]
13. Ramião, N.G.; Martins, P.S.; Rynkevic, R.; Fernandes, A.A.; Barroso, M.; Santos, D.C. Biomechanical properties of breast tissue, a state-of-the-art review. *Biomech. Model. Mechanobiol.* **2016**, *15*, 1307–1323. [CrossRef] [PubMed]
14. Breast Self-Exam. Available online: https://www.breastcancer.org/symptoms/testing/types/self_exam (accessed on 7 July 2018).
15. Elmore, J.G.; Armstrong, K.; Lehman, C.D.; Fletcher, S.W. Screening for breast cancer. *JAMA* **2005**, *293*, 1245–1256. [CrossRef] [PubMed]
16. Higia Technologies. "Eva". Available online: https://www.higia.tech/en/eva (accessed on 11 July 2018).
17. Cyrcadia Health. iT bra. Available online: http://cyrcadiahealth.com/ (accessed on 11 July 2018).
18. Intelligent Artificial Brassiere. CN Patent CN106913320A, 16 March 2017.
19. E-Bra and Methods for Early Detection of Breast Tumor. U.S. Patent WO2013177370A1, 28 November 2013.
20. De Maria, C.; Di Pietro, L.; Lantada, A.D.; Madete, J.; Makobore, P.N.; Mridha, M.; Ravizza, A.; Torop, J.; Ahluwalia, A. Safe innovation: On medical device legislation in Europe and Africa. *Health Policy Technol.* **2018**, *7*, 156–165. [CrossRef]
21. Arti, A.; De Maria, C.; Lantada, A.D.; Di Pietro, L.; Alice, R.; Mannan, M.; Madete, J.; Makobore, P.N.; Aabloo, A.; Kitsing, R.; et al. Towards Open Source Medical Devices-Current Situation, Inspiring Advances and Challenges. *Biodevices* **2018**, *1*, 141–149. [CrossRef]
22. Skovoroda, A.R.; Klishko, A.N.; Gusakyan, D.A.; Mayevskii, Y.I.; Yermilova, V.D.; Oran-skaya, G.A.; Sarvazyan, A.P. Quantitative analysis of the mechanical characteristics of pathologically changed soft biological tissues. *Biophysics* **1995**, *40*, 1359–1364.
23. Krouskop, T.A.; Wheeler, T.M.; Kallel, F.; Garra, B.S.; Hall, T. Elastic moduli of breast and prostate tissues under compression. *Ultrason. Imaging* **1998**, *20*, 260–274. [CrossRef] [PubMed]
24. Zhou, B.; Lukowicz, P. Textile pressure force mapping. In *Smart Textiles*; Springer: Cham, Swizerland, 2017; pp. 31–47. [CrossRef]
25. Mazzei, D.; De Maria, C.; Vozzi, G. Touch sensor for social robots and interactive objects affective interaction. *Sens. Actuators A Phys.* **2016**, *251*, 92–99. [CrossRef]